

Non-contact rack and pinion powered by the lateral Casimir force

Arash Ashourvan,¹ MirFaez Miri,^{1,*} and Ramin Golestanian^{2,†}

¹*Institute for Advanced Studies in Basic Sciences, Zanjan, 45195-1159, Iran*

²*Department of Physics and Astronomy, University of Sheffield, Sheffield S3 7RH, UK*

(Dated: November 20, 2018)

The lateral Casimir force is employed to propose a design for a potentially wear-proof rack and pinion with no contact, which can be miniaturized to nano-scale. The robustness of the design is studied by exploring the relation between the pinion velocity and the rack velocity in the different domains of the parameter space. The effects of friction and added external load are also examined. It is shown that the device can hold up extremely high velocities, unlike what the general perception of the Casimir force as a weak interaction might suggest.

PACS numbers: 07.10.Cm,42.50.Lc,46.55.+d,85.85.+j

With the emergence of the new generation of miniaturized mechanical devices such as micro- and nano-electromechanical systems (NEMS), we have been witnessing a paradigm change in the technical problems involved in making machines and the strategies needed to resolve them. In particular, tribological interactions, i.e. friction, adhesion, and wear, appear to pose new challenges at small length scales [1]. The abundance of surfaces in contact in small devices and high friction are problematic, and the traditional use of lubricants does not work because they become excessively viscous when made into molecular layers [2]. Devices with sliding surfaces in contact are known to wear out too rapidly [3], and it seems that strategies to minimize contact between the surfaces are needed to help make them more durable. The presence of short-ranged attractive dispersion or Casimir forces can cause tiny elements in small devices to stick together and bring the devices to stop [4], and a line of ongoing active research is focused on devising novel techniques to avoid such effects [5, 6]. In light of these technical difficulties, it seems desirable to have novel designs for mechanical devices that can operate without physical contact between their parts.

As a key interaction at nano-scale, Casimir force can be harnessed and used in small devices, as demonstrated by Capasso and collaborators who developed an actuator powered by the normal Casimir force between a flat plate and a sphere [7, 8]. To avoid the limited applicability that the parallel-plate geometry might offer, one can make the two surfaces corrugated and take advantage of a lateral component to the Casimir force, as has been recently proposed [9] and indeed verified experimentally [10]. The lateral Casimir force between corrugated surfaces, provides a possibility for friction-less transduction of lateral forces in nano-mechanical devices without any physical contact between them. The coupling between two surfaces via the quantum vacuum is realized by a term proportional to the sinus of the phase difference between them and is a macroscopic manifestation of quantum coherence, which is reminiscent of the Josephson coupling between superconductors [9, 11]. Because

the coupling is nonlinear, its mechanical response could involve oscillatory and unstable behavior similar to the what is observed in Ref. [8] for the case a device powered by the normal Casimir force.

Here we make use of the lateral Casimir force to design a nano-scale rack and pinion without intermeshing, as shown in Fig. 1a. Our system consists of a corrugated plate (rack) and a corrugated cylinder (pinion) that are kept at a distance from each other. The pinion could be subject to external load (see Fig. 1b), and could experience friction when rotating around its axis. For uniform motion of the rack with a velocity V_R , we find that the “contact” pinion velocity V_P (see Fig. 1a) is locked in to the rack velocity for sufficiently small values of V_R , and that there is a threshold rack velocity at which the pinion undergoes a *skipping transition* where the pinion can no longer hold the cogs in perfect registry with the rack. In the skipping regime, we find that the average pinion velocity can be both positive and negative (with $V_R > 0$) depending on the initial phase mismatch between the corrugations. The effects of the external load and friction are considered and the regions in the parameter space where the pinion can do work against the load are determined. These studies could help us examine the feasibility and efficiency of such a design as a mechanical

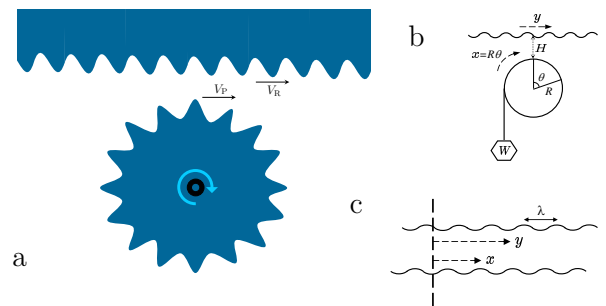


FIG. 1: (a) The rack and pinion with no contact. (b) The schematics of the rack and pinion with an external load W . (c) Two corrugated plates with lateral shift $x - y$. The equilibrium position is at $x = y$.

transducer.

When two sinusoidally modulated plates with identical wavelengths of λ are shifted with respect to each other by a length $x-y$ (see Fig. 1c), the lower plate experience the lateral Casimir force $F_{\text{lateral}} = -F \sin \left[\frac{2\pi}{\lambda}(x-y) \right]$ [9, 11] where the amplitude F depends on the mean separation of the plates and the amplitude of corrugations [10, 12, 13]. The lateral Casimir force introduces a net torque on the pinion, which plays the central role in the equation of motion for the coordinate $x = R\theta$ (Fig. 1b). The equation of motion reads

$$\frac{I}{R} \frac{d^2 x}{dt^2} = -RF \sin \left[\frac{2\pi}{\lambda}(x-y) \right] - \frac{\zeta}{R} \frac{dx}{dt} - RW, \quad (1)$$

where I is the moment of inertia of the pinion about its major axis, ζ is the rotational friction coefficient, and W is an external load against which the pinion should do work.

We focus on the uniform motion of the rack with a velocity V_R , i.e. $y = V_R t$, although similar analyses can be performed for other types of motion such as vibrating [14] or undulating [15] racks, in both of which cases the motion can be rectified. The non-linear equation 1 can be better studied in the phase plane ($u \equiv 2\pi(x-y)/\lambda, v = \dot{u}$), where it reads $\dot{u} = v$, $\dot{v} = -\sin u - \epsilon(v-v_0) - W/F$. In the above equations, we have measured the time in units of $T = \sqrt{I\lambda/(2\pi FR^2)}$, and have defined the dimensionless parameter $\epsilon = T\zeta/I$, which is a measure of the relative importance of friction in the system. The parameter $v_0 = \dot{u}_0 = 2\pi(\dot{x}_0 - V_R T)/\lambda$ is the initial value for v . A key velocity scale is given by

$$V_S = \frac{\lambda}{2\pi T} = \left(\frac{F\lambda R^2}{2\pi I} \right)^{1/2}, \quad (2)$$

which corresponds to the velocity at which the kinetic energy of the rotating pinion is of the order of the work done by the lateral Casimir force upon displacement by one tooth. As we will see below, the quantity $F\lambda$ can be considered as the effective ‘‘bond strength’’ of the coupling between the pinion and rack, so that a ‘‘bound state’’ between them can only tolerate pinion kinetic energies of this order or magnitude, which means that Eq. 2 gives the *skipping velocity*. For simplicity, we only consider the case of pinions that are initially at rest throughout this paper ($\dot{x}_0 = 0$), which means $v_0 = -V_R/V_S$, although the formulation can be readily used to study other initial conditions as well.

No dissipation. In the absence of dissipation and load, Eq. 1 is identical to the celebrated nonlinear plane pendulum problem [16]. It is well known that for this system, the ‘‘energy’’ $h = \frac{1}{2}v^2 + 1 - \cos u = \frac{1}{2} \left(\frac{V_R}{V_S} \right)^2 + 1 - \cos u_0$, is a constant of motion, and there are two families of periodic orbits, corresponding to rotations ($h > 2$) and oscillations ($h < 2$). For $0 < h < 2$,

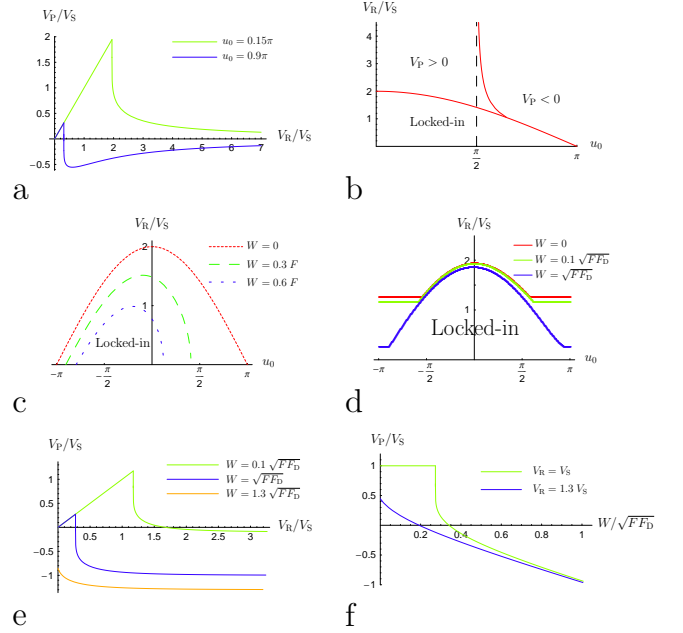


FIG. 2: (a) Pinion velocity versus rack velocity in the absence of dissipation and external load. (b) Domains of positive and negative pinion velocities as well as the phase boundary for the skipping transition. Only half of the plot is shown due to $u_0 \rightarrow -u_0$ symmetry in this case. (c) Phase boundary for the skipping transition, in the absence of dissipation, as a function of the external load. (d) Phase boundary for the skipping transition, in the presence of weak dissipation, as a function of the external load for $\sqrt{F_D}/F = 0.05$. (e) Pinion velocity versus rack velocity in the presence of weak dissipation and external load. (f) Force-velocity response of the rack and pinion could be of two general forms depending on the value of the rack velocity.

the system is oscillatory with a period of $4K(\sqrt{h/2})$, where $K(m) = \int_0^{\pi/2} d\theta (1 - m^2 \sin^2 \theta)^{-1/2}$ is the complete elliptic integral of the first kind [17]. In this case $|u| \leq |\cos^{-1}(1-h)| \leq \pi$, which means that the distance $|x-y|$ between the teeth of the rack and pinion does not exceed $\lambda/2$. Thus the pinion is locked-in with the rack and will have a forward motion with superimposed oscillations (jerks). In the case of $h > 2$, the system is not locked in any more and depending on the initial conditions it can have different behaviors.

The value of h , which determines the behavior of the system, depends on V_R and u_0 . For $V_R < V_S \sqrt{2(1 + \cos u_0)}$ the rack and pinion are geared up and we have $V_P = V_R$ for the jerk-averaged pinion velocity. Higher rack velocities $V_R > V_S \sqrt{2(1 + \cos u_0)}$ cause the system to go to the ‘‘rotation’’ phase of the equivalent pendulum problem, which means that the pinion skips teeth with respect to the rack, but will still have a net average velocity that can be calculated as

$$V_P = V_R - \frac{\pi V_S}{\sqrt{2/h} K(\sqrt{2/h})}, \quad (3)$$

In Fig. 2a, the pinion velocity is plotted as a function of the rack velocity for two values of the initial phase mismatch. The pinion velocity rises linearly with the rack velocity initially and then drops abruptly at the skipping transition. At large rack velocities $V_R \gg V_S$, the pinion velocity has an asymptotic form $V_P = \cos u_0 V_S^2 / V_R + \dots$, which shows that it vanishes at infinity, and that the decay can be both from below (for $u_0 > \pi/2$) and above (for $u_0 < \pi/2$). An intriguing feature here is the possibility of dropping into negative pinion velocities—the *reverse gear*—after the skipping transition, as Fig. 2a shows. Figure 2b delineates the different domains of phase lock-in, forward motion, and reverse motion, in the space of the rack velocity and the phase mismatch. One can see that for $0 < u_0 < \pi/2$ the average velocity is always positive, while for $\pi/2 < u_0 < \pi$ the pinion velocity can be switched from positive to negative by increasing V_R/V_S . This can be achieved by either speeding up the rack or decreasing the skipping velocity by increasing the separation between the rack and pinion (see below).

The effect of external load. In the absence of dissipation, Eq. 1 has $h' = v^2/2 + 1 - \cos u + Wu/F$ as the constant of motion. Two classes of motion are separated by the saddle-loop of energy $h'_s = 1 + \sqrt{1 - (W/F)^2} - [\pi - \sin^{-1}(W/F)](W/F)$, leading to rotations for $h' > h'_s$ and oscillations for $h' < h'_s$, in the equivalent pendulum problem. Figure 2c shows the domains for two different regimes as well as the boundary for the skipping transition as a function of the rack velocity and the initial phase mismatch. As the load is increased, the two fixed point approach each other thereby narrowing down the locked-in region, until at $W = F$ it disappears when they fully merge. Therefore, $W < F$ is a necessary condition to have positive rack velocities.

Weak dissipation. The dynamical system described by Eq. 1 is not integrable in the presence of the dissipation term, as energy is not conserved. If the dissipation is weak, such that $\zeta V_R/R^2 + W < F$, we can use the Melnikov method [16, 18] to study the perturbed phase portrait of the system. In this regime, the force scale $F_D = \frac{\zeta^2 \lambda}{2\pi I R^2}$ seems to play an important role. (Note that $\zeta V_S/R^2 = \sqrt{F F_D}$.)

Similar to the dissipation-free case, the system develops the two classes of commensurate and incommensurate motion transduction separated by a skipping transition boundary. Figure 2d shows an example of this phase diagram that has been calculated numerically, for different values of the external load. The phase boundary consists of horizontal (u_0 -independent) parts that are met by a bell-shaped central part. In the part that does not depend on u_0 , we find that for $\zeta V_R/R^2 < \frac{4}{\pi} \sqrt{F F_D} - W$ the system is in the locked-in phase and we have $V_P = V_R$. As the rack velocity is increased above this limit, the system undergoes a skipping transition. The pinion velocity for $\zeta V_R/R^2 > \frac{4}{\pi} \sqrt{F F_D} - W$ can be found from Eq. 3, with a value $h = h_m$ that is a solution to this

equation $V_R + WR^2/\zeta = \frac{4}{\pi} V_S \sqrt{h_m/2} E\left(\sqrt{2/h_m}\right)$ with $E(m) = \int_0^{\pi/2} d\theta \sqrt{1 - m^2 \sin^2 \theta}$ being the complete elliptic integral of the second kind [17]. Figure 2e shows the pinion velocity as a function of the rack velocity for different values of the external load. The general feature of a drastic drop in the pinion velocity after the skipping transition is observed, and the asymptotic behavior $V_P = -WR^2/\zeta + \frac{1}{2} V_S^4 / V_R^3 + \dots$, at large rack velocities shows a complete decoupling in the system at infinitely large V_R . The response of the system in the bell-shaped region of the phase diagram of Fig. 2d leads to similar results and can be obtained numerically. Note that the Melnikov approximation breaks down for large rack velocities and we need a complementary approach to examine the behavior of the system in that limit (see below).

The force-velocity response of the system in the u_0 -independent region can also be extracted from this result. Figure 2f shows the pinion velocity as a function of the external load for two values of the rack velocity. For $V_R < \frac{4}{\pi} V_S$, the pinion velocity is independent of the load for $W < \frac{4}{\pi} \sqrt{F F_D} - \zeta V_R/R^2$, and drops drastically after the onset of skipping, whereas the decrease upon introduction of load starts from the beginning when $V_R > \frac{4}{\pi} V_S$. One can identify the load at which the pinion velocity vanishes as the *stall force*.

Strong dissipation. The Melnikov method fails if $\zeta V_R/R^2 + W \gtrsim F$, but in this limit we can proceed by neglecting the acceleration term $\dot{v} = \ddot{u}$ in Eq. 1. This allows us to solve the equation in closed form, which yields $u(t) = 2 \tan^{-1} \left[\left(\frac{F}{\zeta V_R/R^2 + W} \right) - \sqrt{1 - \left(\frac{F}{\zeta V_R/R^2 + W} \right)^2} \tan \left(\frac{\pi t}{\tau} \right) \right]$, where $\tau = \lambda / \sqrt{(V_R + WR^2/\zeta)^2 - (FR^2/\zeta)^2}$. The explicit expression for u can be used to calculate the time-averaged pinion velocity $V_P = V_R - \sqrt{(V_R + WR^2/\zeta)^2 - (FR^2/\zeta)^2}$ which produces very similar curves to those plotted in Fig. 2e above the skipping transition (using the Melnikov method). The stall force (load) in this limit can be found as $W_s = F \left[\sqrt{1 + (\zeta V_R/FR^2)^2} - (\zeta V_R/FR^2) \right]$.

To make a stronger link to the experiments, we need to quantify the amplitude of the lateral Casimir force F . For a cylinder of radius R located at a (nearest) distance H from a plate (see Fig. 1b), the Casimir interaction can be calculated from the corresponding interaction between two parallel plates, using the Proximity Force Approximation (PFA) [19]. For the normal Casimir force between perfect metals, it has been recently shown that this approximation works surprisingly well for $H \lesssim R$ [20]. Using PFA for the lateral Casimir force between a pinion of length L and corrugation amplitude a_1 and a rack of corrugation amplitude a_2 with $a_1, a_2 \ll H$, we

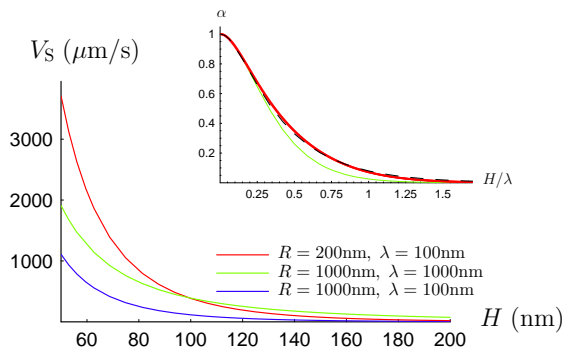


FIG. 3: Skipping velocity as a function of the gap size for perfect metallic boundaries, corresponding to $\rho = 19.3 \text{ gr/cm}^3$ (gold) and $a_1 = a_2 = 10 \text{ nm}$, for different values of radius and corrugation wavelength. Inset: the parameter α introduced in the text as a function of H/λ for perfect metals (red dots) compared to the pairwise summation approximation (green solid line). The dashed-line shows the empirical formula presented in the text.

find

$$F = \left(\frac{7\pi^4\sqrt{2}}{3072} \right) \frac{\hbar c a_1 a_2 L R^{1/2}}{\lambda H^{9/2}} \alpha \left(\frac{H}{\lambda} \right), \quad (4)$$

to the leading order, where $\alpha = \frac{3072}{7\pi^3} \int_1^\infty \frac{dt}{t^5 \sqrt{t-1}} J \left(\frac{H}{\lambda} t \right)$ with J being the (“Josephson–”) coupling function presented in Ref. [12]. The inset of Fig. 3 shows the dependence of α on H/λ for perfect metals and a comparison to pairwise summation approximation, with the dashed-line showing an empirical approximate formula $\alpha_e = 1/\cosh^{4/9} \left(\frac{12\pi}{\sqrt{35}} \frac{H}{\lambda} \right)$ which could be useful for practical purposes. Using this result we find

$$V_S = \left(\frac{7\pi^2\sqrt{2}}{3072} \right)^{1/2} \left(\frac{\hbar c}{\rho H^4} \right)^{1/2} \left(\frac{a_1 a_2}{H^2} \right)^{1/2} \left(\frac{H}{R} \right)^{3/4} \alpha^{1/2}, \quad (5)$$

where ρ is the mass density of the pinion. This result shows a strong power law behavior at small values of H followed by an exponential decay at large H whose length scale is set by λ . Figure 3 shows the skipping velocity as a function of the gap size, for different values of the radius and wavelength. The typical values for V_S , which correspond to velocities that the system could transfer robustly, are remarkably high: translated into angular velocity they are in the kHz region. The strong dependence of the skipping velocity on the gap size can be used to explore the parameter space and change the behavior of the system. For example, one can reduce V_S —move in the vertical direction in the phase diagram of Fig. 2b—by increasing H , and thus switch the system from the locked-in phase to a reverse gear, at constant rack velocity. In other words, changing the separation provides a continuous analogue of the clutch–gear system. The calculations presented here have been based on

the assumption of perfect metallic boundaries, and one expects corrections for gap sizes smaller than the plasma wavelength of the metals [13].

The value of the friction coefficient ζ is also instrumental in determining the behavior of the system. While this quantity is highly system-dependent in general, it is interesting to note that a contribution to dissipation also comes from the interplay between the electromagnetic fluctuations and the dielectric loss properties of the two objects [21].

In conclusion, we have proposed a design for a nano-scale rack and pinion without contact by employing the quantum fluctuations of the electromagnetic field. This design, and the corresponding variants that could be readily conceived, might help towards making more durable machine parts for small mechanical system.

This work was supported by EPSRC under Grant EP/E024076/1 (R.G.).

* Electronic address: miri@iasbs.ac.ir

† Electronic address: r.golestanian@sheffield.ac.uk

- [1] R.W. Carpick, *Science* **313**, 184 (2006).
- [2] Y.Z. Hu and S. Granick, *Trib. Lett.* **5**, 81 (1998).
- [3] M.P. de Boer, T.M. Mayer, *MRS Bull.* **26**, 302 (2001).
- [4] E. Buks and M.L. Roukes, *Phys. Rev. B* **63**, 033402 (2001).
- [5] A. Socoliuc, E. Gnecco, S. Maier, O. Pfeiffer, A. Baratoff, R. Bennowitz, E. Meyer, *Science* **313**, 207 (2006).
- [6] J.Y. Park, D.F. Ogletree, P.A. Thiel, and M. Salmeron, *Science* **313**, 186 (2006).
- [7] H.B. Chan, V. A. Aksyuk, R. N. Kleiman, D. J. Bishop and F. Capasso, *Science* **291**, 1941 (2001).
- [8] H.B. Chan, V. A. Aksyuk, R. N. Kleiman, D. J. Bishop and F. Capasso, *Phys. Rev. Lett.* **87**, 211801 (2001).
- [9] R. Golestanian and M. Kardar, *Phys. Rev. Lett.* **78**, 3421 (1997).
- [10] F. Chen, U. Mohideen, G.L. Klimchitskaya, and V.M. Mostepanenko, *Phys. Rev. Lett.* **88**, 101801 (2002).
- [11] R. Golestanian and M. Kardar, *Phys. Rev. A* **58**, 1713 (1998).
- [12] T. Emig, A. Hanke, R. Golestanian, and M. Kardar, *Phys. Rev. A* **67**, 022114 (2003).
- [13] R.B. Rodrigues, P.A. Maia Neto, A. Lambrecht, and S. Reynaud, *Phys. Rev. Lett.* **96**, 100402 (2006).
- [14] A. Ashourvan, M.F. Miri, and R. Golestanian, unpublished.
- [15] T. Emig, private communication.
- [16] J. Guckenheimer and P. Holmes, *Nonlinear Oscillations, Dynamical Systems, and Bifurcations of Vector Fields* (Springer-Verlag, Berlin, 1983).
- [17] I.S. Gradshteyn and I. M. Ryzhik, *Table of Integrals, Series, and Products*, 6th edition (Academic Press, New York, 2000).
- [18] V.K. Melnikov, *Trans. Moscow Math. Soc.* **12**, 1 (1963).
- [19] B. Derjaguin, *Kolloid-Z.* **69**, 155 (1934).
- [20] T. Emig, R.L. Jaffe, M. Kardar, and A. Scardicchio, *Phys. Rev. Lett.* **96**, 080403 (2006).
- [21] J.B. Pendry, *J. Phys.: Condens. Matter* **9** 10301 (1997).